Second-harmonic generation imaging of collagen fibers in myocardium for atrial fibrillation diagnosis

Ming-Rung Tsai
National Taiwan University
Graduate Institute of Photonics and Optoelectronics
and
Department of Electrical Engineering
1 Roosevelt Road Section 4
Taipei, 10617 Taiwan

Yu-Wei Chiu
Far-Eastern Memorial Hospital
Division of Cardiology
Department of Internal Medicine
21 Nan-Ya South Road Section 2
Pan-Chiao 22060, Taiwan

Men Tzung Lo
National Central University
Research Center for Adaptive Data Analysis
300 Jhongda Road
Chungli 32001, Taiwan

Chi-Kuang Sun
National Taiwan University
Graduate Institute of Photonics and Optoelectronics
and
Department of Electrical Engineering
1 Roosevelt Road Section 4
Taipei, 10617 Taiwan
and
Academia Sinica
Research Center for Applied Sciences
128 Academia Road Section 2
Taipei 11529, Taiwan

Abstract. Atrial fibrillation (AF) is the most common irregular heart rhythm and the mortality rate for patients with AF is approximately twice the mortality rate for patients with normal sinus rhythm (NSR). Some research has indicated that myocardial fibrosis plays an important role in predisposing patients to AF. Therefore, realizing the relationship between myocardial collagen fibrosis and AF is significant. Second-harmonic generation (SHG) is an optically nonlinear coherent process to image the collagen network. We perform SHG microscopic imaging of the collagen fibers in the human atrial myocardium. Utilizing the SHG images, we can identify the differences in morphology and the arrangement of collagen fibers between NSR and AF tissues. We also quantify the arrangement of the collagen fibers using Fourier transform images and calculating the values of angle entropy. We indicate that SHG imaging, a nondestructive and reproducible method to analyze the arrangement of collagen fibers, can provide explicit information about the relationship between myocardial fibrosis and AF. © *2010 Society of Photo-Optical Instrumentation Engineers.* [DOI: 10.1117/1.3365943]

Keywords: second-harmonic generation; collagen; atrial fibrillation; Fourier transform image.

Paper 09324P received Aug. 18, 2009; accepted for publication Jan. 8, 2010; published online Mar. 25, 2010.

1 Introduction

Atrial fibrillation (AF) is the most common arrhythmia and affects more than 2.3 million Americans. Patients with AF suffer from many risks, such as tachycardia-induced atrial dysfunction, cardiomyopathy, thromboembolism, and stroke.[1] Proper balance between synthesis and degradation of extracellular matrix molecules is critical for maintaining normal physiologic function. In the human atrial myocardium, the major component of the extracellular matrix is collagen fibers.[2] Recently, many studies[3–5] have observed structural remodeling of the extracellular collagen matrix and collagen fibrosis in atrial diseases such as AF. However, the detailed mechanism of AF is still not fully realized and limited reports are available on the relationship between myocardial fibrosis and AF.

Characteristic changes in the organization of fibrillar collagen are known to occur in several diseases[6,7] and could potentially serve as an early diagnostic marker. We propose that collagen fibrosis in the human atrium myocardium is involved in the development of AF. It is desired to find a simple and reproducible method to obtain information concerning collagen fibers for quantitative analysis. Many methods can be used to quantify collagen fibers, such as the weight measurement method[8] and the colorimetric method.[9] But these methods necessitate destroying the structure of the tissues and the tissues can not be used for further analysis (for example, pathohistological analysis). Optical imaging techniques, such as confocal microscopy[10] and second-harmonic generation (SHG) microscopy[11] can quantify collagen fibers as well. However, utilizing the confocal microscopy, the tissues must be stained and are still destroyed. Non-fluorescence-based SHG microscopy uses IR excitation wavelengths that minimize the energy deposition and increase the tissue penetration while maintaining intrinsically high spatial resolution without staining.[12] Since 1986,[13] SHG has emerged as a powerful biological imaging modality for biotissues.[14–24] However, using SHG microscopy for myocardium observation has never been

Address all correspondence to: Chi-Kuang Sun, National Taiwan University, Photonics and Optoelectronics R319, 2nd EE Building, 1 Roosevelt Road Section 4 Taipei, 10617 Taiwan. Tel: 886-2-33665085; Fax: 886-2-33663614; E-mail: sun@cc.ee.ntu.edu.tw.

1083-3668/2010/15(2)/026002/6/$25.00 © 2010 SPIE

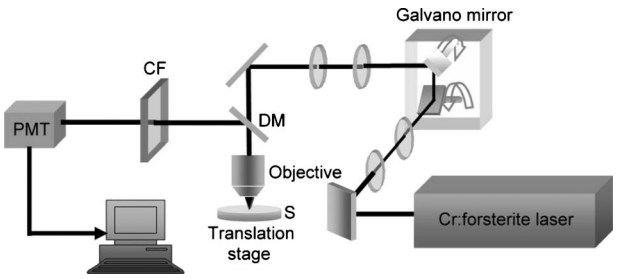

Fig. 1 Schematic diagram of an SHG microscope: PMT, photomultiplier tube; CF, color filter; DM, dichroic mirror; S, sample.

reported. In this paper, we apply SHG microscopy for collagen fiber imaging in human atrial myocardium samples. Utilizing the SHG images, we can identify the differences in morphology and arrangement of collagen fibers between normal sinus rhythm (NSR) and AF tissues. We further quantify the arrangement of the collagen fibers by using Fourier transform images and calculating the values of angle entropy. Our study indicates that collagen fibrosis in human atrium myocardium is indeed involved in the development of AF. Our study also demonstrates that SHG imaging, a nondestructive and reproducible method to analyze the arrangement of collagen fibers, can provide explicit information about the relationship between myocardial fibrosis and AF and can serve potentially as an early diagnostic marker for AF.

2 Methods and Materials

2.1 *SHG Microscopy*

The first biological imaging experiment using SHG microscopy to study the orientation of collagen fibers was done by Freund et al.[13] in 1986. Recently, SHG has been applied in different biotissues consisting of tendon,[14] bone,[15] tubulin,[16,17] muscle fibers,[18–23] zona pellucida,[24] strain in enamel rods,[25] and polyhedral inclusion bodies of viruses.[26] Collagen fiber has a highly crystalline triple-helix structure that is not centrosymmetric. Thus, SHG microscopy is an ideal tool to observe collagen fiber structure.[16,18,27–31] The heart structure is also an interesting subject for SHG imaging to increase understanding of heart disease, including heart valves,[32,33] and cardiac myocytes.[34–36] In the human atrial myocardium, the major components are cardiac muscles and collagen fibers; hence, we utilized SHG microscopy to image the human atrial myocardium. Figure 1 shows the experimental setup of the SHG microscope. The excitation light source was a home-built Cr:forsterite laser that operates at 1230 nm with a pulse width of 140 fs, a repetition rate of 110 MHz, and 450 mW of average output. The Cr:forsterite laser was pumped by 10 W of 1064 nm light from a diode-pumped $Nd:YVO_4$ laser. All optics were modified to enable the passage of the excitation source light. We adapted the high-speed galvanometer mirrors (GMs) inside the FV300 scanning system with a BX51 upright microscope and a high-numerical-aperture (NA) objective (LUMPlanFl/IR 60×/water/NA 0.90), all from Olympus. Real-time SHG images can be obtained by using a photomultiplier tube (PMT). CF is color filter to filter the excitation light, DM is the dichroic mirror, and S is the sample, which is mounted on the translation stage to form 2-D sectioned images.

2.2 *Fourier Transform Image Analysis*

The Fourier transform is an important image processing tool that has also been used to determine the orientation and anisotropy of the microstructure, such as collagen fibers.[37–39] Many studies have combined SHG microscopy and a Fourier transform to analyze the orientation or periodicity of the studied biological structures, such as skeletal muscle,[40] corneal tissues,[41] and collagen gels.[42] We Fourier transformed the SHG images to obtain the spatial distribution characteristics of collagen fibers in the human atrial myocardium. The acquired SHG image is composed of 512×512 pixels and each pixel can be considered as a spatial function $f(x,y)$, representing the image intensity at a point (x,y), while its spatial Fourier transform is defined by

$$F(u,v) = \int_{-\infty}^{\infty} \int_{-\infty}^{\infty} f(x,y) \exp[-i2\pi(ux+vy)] \mathrm{d}x\, \mathrm{d}y, \quad (1)$$

where x and y represent the spatial coordinates of the image; and u and v indicate the spatial frequency components along x and y, respectively, in the Fourier domain. Therefore, each spatial Fourier transform function $F(u,v)$ is regarded as a pixel intensity value at a point (u,v) to form a Fourier image (512×512 pixels) in the Fourier domain. Moreover, to obtain more explicit information about collagen arrangement, we calculated the angle entropy from the Fourier transform images. The probability of the distribution function P_s is given by

$$S(\phi) = \int F(\omega, \phi) \mathrm{d}\omega, \quad (2)$$

where the distribution function S in the Fourier domain in polar coordinates is defined by

$$P_{S(\phi)} = \frac{S(\phi)}{\int S(\phi) \mathrm{d}\phi}. \quad (3)$$

Then the angle entropy H is calculated as

$$H = -\int P_{S(\phi)} \ln P_{s(\phi)} \, \mathrm{d}\phi. \quad (4)$$

Finally, the angle entropy can be obtained. We get the Fourier images and the values of the angle entropy according to preceding equations and these analyses were performed with MATLAB.[43]

2.3 *Materials*

The study group consists of 10 patients with AF and 10 patients with NSR. All patients received open heart surgery with valvular heart disease and their age was more than 18 years. Exclusion criteria include patients with cardiogenic shock, patients receiving major surgery within past 6 weeks, patients with concomitant infection, patients with abnormal liver function, and pregnant women. Atrial tissues from all patients were obtained from the right atrium and were cut into sections

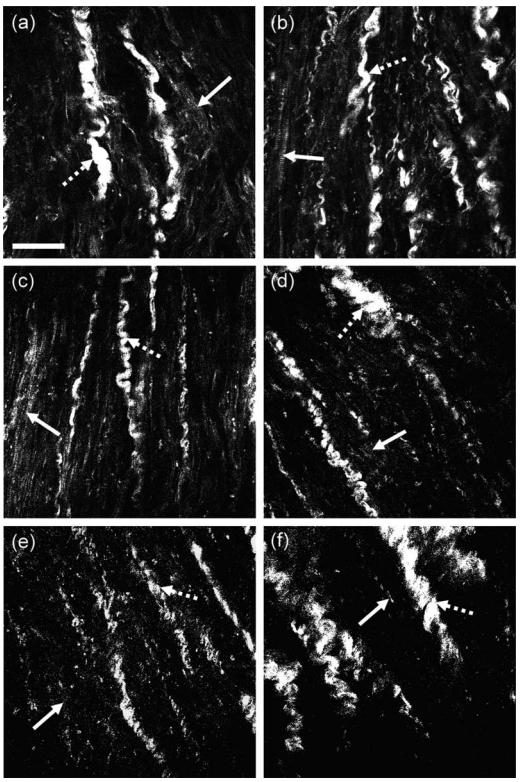

Fig. 2 (a) to (f) SHG images of the atrial myocadia from patients with NSR. The arrangements of the collagen fibers (dashed arrows) are regular and directional to a specific angle. The cardiac muscles (solid arrows) can also be observed. (Scale bar: 50 μm)

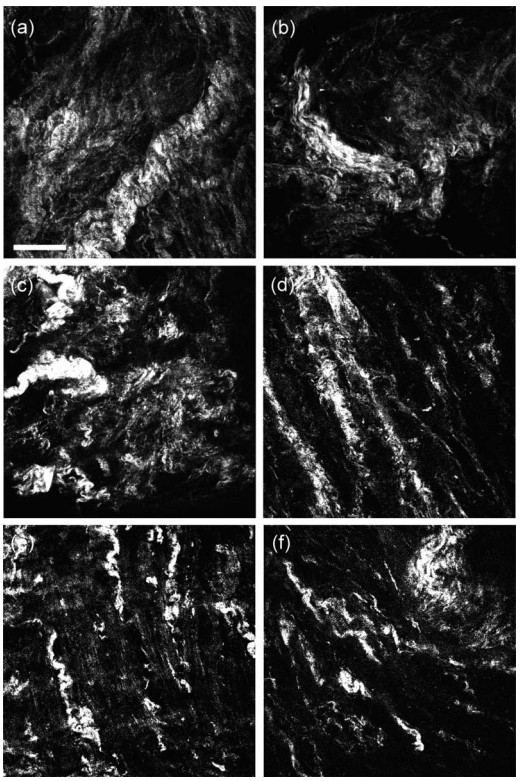

Fig. 3 (a) to (f) SHG images of the atrial myocadia from patients with AF. The collagen fibers are found to be entangled and the arrangements in AF tissues are less orderly than in NSR tissues. Collagen fibrosis can be observed. (Scale bar: 50 μm)

with about 5 mm thicknesses. The specimens were incubated directly into optimal cutting temperature (OCT) compound at temperature −20 °C until we observed these samples by using the SHG microscope at room temperature. The Ethics Committee of National Taiwan University Hospital approved the study and all patients provided written informed consent.

3 Results and Discussion

3.1 *Epi-SHG Images of Human Atrial Myocardium*

The human atrial myocardium samples for SHG imaging study were received by open heart surgery and were cut into sections with approximately 5 mm thicknesses. The heart consists of three layers: epicardium, myocardium, and endocardium, and the cardiac muscles exist only in the myocardium. Thus, by observing the collagen fibers and cardiac muscles simultaneously, we can make sure that we observed the collagen fibers in the myocardium, not in the epicardium nor in the endocardium. Because SHG is sensitive to collagen fibers and cardiac muscle fibers, the arrangement of collagen fibers in the atrial myocardium can be revealed by SHG images. Figures 2(a)–2(f) show the SHG images taken in the atrial myocardia from different patients with NSR. The orderly arranged collagen fibers can be found to be parallel to the cardiac muscles in the same layer. We also can observe the different epi-SHG intensities between collagen fibers and muscle fibers. The epi-SHG intensity from collagen fibers is observed to be about 3 to 10 times that from muscle fibers and a similar result in skeletal muscles were revealed due to phase matching and the thickness of the tissues.[44] In contrast, the SHG images of the atrial myocardia from different AF patients are shown in Figs. 3(a)–3(f). The collagen fibers are found to be entangled and the arrangements in AF tissues are less orderly than in NSR tissues. Clear differences in collagen fiber arrangements between NSR and AF tissues can be revealed by comparing Fig. 2 with Fig. 3.

3.2 *Histological Results of the Human Atrial Myocardium*

After obtaining the SHG images of the atrial myocardium, the specimens were fixed in formalin and were stained with Masson's trichrome. The sections of the atrial myocardium with the Masson's trichrome stain by using the bright-field microscope are shown in Fig. 4(a) for NSR and in Fig. 4(b) for AF tissues. The dashed and solid arrows indicate the positions of the collagen fibers and the cardiac muscles, respectively. From Fig. 4(a), the collagen fibers in NSR tissues reveal orderly arrangement and are parallel to the cardiac muscles. Figure 4(b) shows the entangled and disoriented arrangement of the collagen fibers in AF tissues. The conclusion from the histological results is consistent with the SHG images as shown in Figs. 2 and 3 and shows that the structures of the human myocardium, including collagen fibers and cardiac muscles, can be revealed with SHG microscopy.

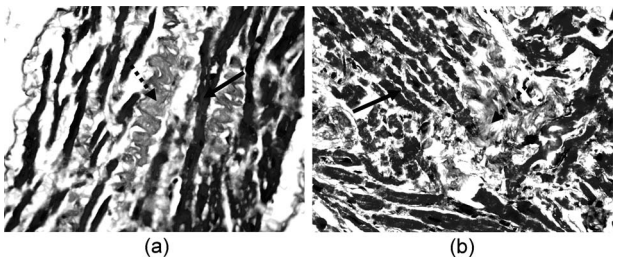

Fig. 4 Sections of the atrial myocardium with the Masson's trichrome stain by using the bright-field microscope for (a) NSR and (b) AF tissues. The collagen fibers (dashed arrow) in NSR tissues show an orderly arrangement and are parallel to cardiac muscles (solid arrow). The entangled and disoriented arrangement of the collagen fibers is revealed in AF tissues and the results are consistent with SHG images.

3.3 *Fourier Transform Analysis*

A Fourier transform is an ideal tool to determine the orientation and anisotropy of the collagen fibers. Utilizing a Fourier transform to analyze SHG images, the arrangement of collagen fibers can be quantified without depending on the intensities of the SHG images. We Fourier transformed the SHG images into the spatial frequency domain following Eq. (1). The epi-SHG signals from muscle fibers are weaker than those from collagen fibers and we want to analyze only the collagen fiber arrangement. Thus, we set a threshold value of the SHG intensity, and the signals from muscle fibers can be filtered before taking Fourier transform if the SHG intensities are lower than the threshold value. The Fourier images of the SHG images of the atrial myocadia are shown in Fig. 5(a) for NSR and in Fig. 5(b) for AF tissues. As mentioned, the arrangement of the collagen fibers in NSR tissues is more orderly, hence the distribution of the Fourier image shows a directional pattern in Fig. 5(a). The Fourier SHG image of AF tissues presents a nondirectional pattern due to randomized arrangement of the collagen fibers, as exampled in Fig. 5(b).

Furthermore, the arrangement of collagen fibers can be quantified by calculating the angle entropy from the Fourier transform images. To obtain the differences of the collagen fiber arrangements between NSR and AF tissues, we calculated the angle entropy according to the formula in Sec. 2.2 to quantify the arrangement of the collagen fibers in the atrial myocardium. The total number of over 500 SHG images of NSR and AF tissues (279 data for NSR and 251 data for AF) were analyzed. The distribution of angle entropy is shown in a histogram in Fig. 6, where the mean values of the analyzed angle entropy for the NSR and AF tissues are 2.82 ± 0.40 and 3.79 ± 0.47, respectively. The entropy is a measure of the disorder in the arrangement of the microstructure and the higher the entropy the greater the disorder.[45] Therefore, the value of angle entropy indicates that the collagen fiber arrangement in AF tissues is much more disordered than in NSR tissues. The result suggests that we succeeded in obtaining the quantification of collagen fiber arrangement by using the Fourier analysis of SHG images and the collagen fibrosis in the atrial myocardium is implicated in the existence of AF.

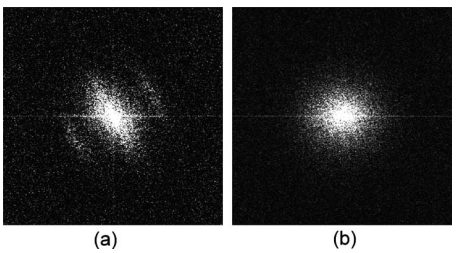

Fig. 5 Fourier transform images of the SHG images in atrial myocadia for (a) NSR and (b) AF tissues. The arrangement of the collagen fibers in NSR tissues is more orderly, hence the Fourier transform images shows a directional pattern. In contrast, the Fourier transform images in AF tissues present a nondirectional pattern due to randomized arrangement of the collagen fibers.

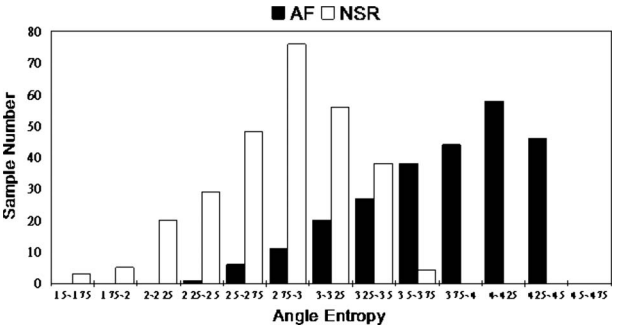

Fig. 6 Distribution of the angle entropy for NSR and AF tissues. The mean values of angle entropy for the NSR and AF tissues are 2.82 ± 0.40 and 3.79 ± 0.47, respectively. The values of the angle entropy indicate that the arrangement in AF tissues is more disordered than in NSR tissues.

4 Conclusion

We proposed that collagen fibrosis in the human atrium myocardium is involved in the development of AF; thus, it was significant to find a simple and reproducible method to obtain the information about the collagen fibrosis. SHG could provide strong contrasts in the collagen fibers and cardiac muscle fibers of the human atrial myocardium. Thus, the epi-SHG intensities from collagen fibers are stronger than those from muscle fibers and the different arrangements of collagen fibers between NSR and AF tissues were revealed. Furthermore, we quantified the collagen fiber arrangement by using a Fourier transform and calculating angle entropy. The Fourier transform images show the nondirectional and directional patterns in AF and NSR tissues, respectively. By analyzing the Fourier transform images, the angle entropy was calculated. As expected, the higher angle entropy was obtained in AF tissues. We succeeded for the first time in quantifying the arrangement of collagen fibers of the human atrial myocardium in normal and disease states. These results indicate that the random arrangement of collagen fibers in AF tissues and collagen fibrosis in the human atrium myocardium is involved in the development of AF. Therefore, SHG microscopy can serve as a noninvasive tool for collagen fibrosis imaging in the human atrium myocardium and can be an ideal tool for AF diagnosis in the future.

Acknowledgments

This research is sponsored by the National Health Research Institute of Taiwan (Grant No. NHRI-EX99-9936EI), the Na-

tional Taiwan University (Grant No. NTU 98R0036-01), the National Science Council (Grant No. NSC 97-2314-B-002-139), the Far-Eastern Memorial Hospital (Grant No. FEMH-96-C-019), and the National Taiwan University Research Center for Medical Excellence. M-T Lo was supported by NSC, Taiwan, Grant No. 98-2627-B-008-005 and joint foundation of CGH and NCU, Grant No. CNJRI-96 CGH-NCU-A3.

References

1. M.-H. Luo, Y.-S. Li, and K.-P. Yang, "Fibrosis of collagen i and remodeling of connexin 43 in atrial myocardium of patients with atrial fibrillation," *Cardiology* **107**, 248–253 (2007).
2. B. Swynghedauw, "Molecular mechanisms of myocardial remodeling," *Physiol. Rev.* **79**, 215–262 (1999).
3. Y.-T. Chiu, T.-J. Wu, H.-J. Wei, C.-C. Cheng, N.-N. Lin, Y.-T. Chen, and C.-T. Ting, "Increased extracellular collagen matrix in myocardial sleeves of pulmonary veins: an additional mechanism facilitating repetitive rapid activities in chronic pacing-induced sustained atrial fibrillation," *J. Cardiovasc. Electrophysiol.* **16**, 753–759 (2005).
4. S. Kostin, G. Klein, Z. Szalay, S. Hein, E. P. Bauer, and J. Schaper, "Structural correlate of atrial fibrillation in human patients," *Cardiovasc. Res.* **54**, 361–379 (2002).
5. A. Boldt, U. Wetzel, J. Lauschke, J. Weigl, J. Gummert, G. Hindricks, H. Kottkamp, and S. Dhein, "Fibrosis in left atrial tissue of patients with atrial fibrillation with and without underlying mitral valve disease," *Heart* **90**, 400–405 (2004).
6. H. D. Intengan and E. L. Schiffrin, "Vascular remodeling in hypertension—Roles of apoptosis, inflammation, and fibrosis," *Hypertension* **38**, 581–587 (2001).
7. R. Bataller and D. A. Brenner, "Liver fibrosis," *J. Clin. Invest.* **115**, 209–218 (2005).
8. D. Taskiran, E. Taskiran, H. Yercan, and F. Z. Kutay, "Quantification of total collagen in rabbit tendon by the Sirius red method," *Tr. J. Medical Sciences* **29**, 7–9 (1999).
9. R. Valderrama, S. Navarro, E. Campo, J. Camps, A. Gimenez, A. Parés, and J. Caballeria, "Quantitative measurement of fibrosis in pancreatic tissue," *Int. J. Pancreatol.* **10**, 23–29 (1991).
10. A. J. Pope, G. B. Sands, B. H. Smaill, and I. J. LeGrice, "Three-dimensional transmural organization of perimysial collagen in the heart," *Am. J. Physiol. Heart Circ. Physiol.* **295**, H1243–H1252 (2008).
11. O. Nadiarnykh, S. Plotnikov, W. A. Mohler, I. Kalajzic, D. Redford-Badwal, and P. J. Campagnola, "Second harmonic generation imaging microscopy studies of osteogenesis imperfecta," *J. Biomed. Opt.* **12**, 051805 (2007).
12. C.-K. Sun, S.-W. Chu, S.-Y. Chen, T.-H. Tsai, T.-M. Liu, C.-Y. Lin, and H.-J. Tsai, "Higher harmonic generation microscopy for developmental biology," *J. Struct. Biol.* **147**, 19–30 (2004).
13. I. Freund, M. Deutsch, and A. Sprecher, "Connective tissue polarity. Optical second harmonic generation microscopy, crossed-beam summation, and small-angle scattering in rat tail tendon," *Biophys. J.* **50**, 693–712 (1986).
14. P. Stoller, B.-M. Kim, A. M. Rubinchik, K. M. Reiser, and L. B. Da Silva, "Polarization-dependent optical second-harmonic imaging of a rat-tail tendon," *J. Biomed. Opt.* **7**, 205–214 (2002).
15. W. Mohler, A. C. Millard, and P. J. Campagnola, "Second harmonic generation imaging of endogenous structural proteins," *Methods* **29**, 97–109 (2003).
16. P. J. Campagnola, A. C. Millard, M. Terasaki, P. E. Hoppe, C. J. Malone, and W. A. Mohler, "3-dimensional high-resolution second harmonic generation imaging of endogenous structural proteins in biological tissues," *Biophys. J.* **82**, 493–508 (2002).
17. W. R. Zipfel, R. M. Williams, R. Christie, A. Y. Nikitin, B. T. Hyman, and W. W. Webb, "Live tissue intrinsic emission microscopy using multiphoton-excited native fluorescence and second harmonic generation," *Proc. Natl. Acad. Sci. U.S.A.* **100**, 7075–7080 (2003).
18. P. J. Campagnola and L. M. Loew, "Second-harmonic imaging microscopy for visualizing biomolecular arrays in cells, tissues and organisms," *Nat. Biotechnol.* **21**, 1356–1360 (2003).
19. W.-L. Chen, T.-H. Li, P.-J. Su, C.-K. Chou, P.-T. Fwu, S.-J. Lin, D. Kim, P.-T. C. So, and C.-Y. Dong, "Second harmonic generation tensor microscopy for tissue imaging," *Appl. Phys. Lett.* **94**, 183902 (2009).
20. M. Both, M. Vogel, O. Friedrich, F. von Wegner, T. Künstung, R. H. A. Fink, and D. Uttenweiler, "Second-harmonic imaging of intrinsic signals in muscle fibers *in situ*," *J. Biomed. Opt.* **9**, 882–892 (2004).
21. F. Vanzi, M. Capitanio, L. Sacconi, C. Stringari, R. Cicchi, M. Canepari, M. Maffei, N. Piroddi, C. Poggesi, V. Nucciotti, M. Linari, G. Piazzesi, C. Tesi, R. Antolini, V. Lombardi, R. Bottinelli, and F. S. Pavone, "New techniques in linear and non-linear laser optics in muscle research," *J. Muscle Res. Cell Motil.* **27**, 469–479 (2006).
22. S.-W. Chu, S.-Y. Chen, G.-W. Chern, T.-H. Tsai, Y.-C. Chen, B.-L. Lin, and C.-K. Sun, "Studies of $\chi^{(2)}/\chi^{(3)}$ tensors in submicron-scaled bio-tissues by polarization harmonics optical microscopy," *Biophys. J.* **86**, 3914–3922 (2004).
23. F. Legare, C. Pfeffer, and B. R. Olsen, "The role of backscattering in SHG tissue imaging," *Biophys. J.* **93**, 1312–1320 (2007).
24. C.-S. Hsieh, S.-U. Chen, Y.-W. Lee, Y.-S. Yang, and C.-K. Sun, "Higher harmonic generation microscopy of *in vitro* cultured mammal oocytes and embryos," *Opt. Express* **16**, 11574–11588 (2008).
25. S.-Y. Chen, C.-Y. S. Hsu, and C.-K. Sun, "Epi-third and second harmonic generation microscopic imaging of abnormal enamel," *Opt. Express* **16**, 11670–11679 (2008).
26. T.-M. Liu, Y.-W. Lee, C.-F. Chang, S.-C. Yeh, C.-H. Wang, S.-W. Chu, and C.-K. Sun, "Imaging polyhedral inclusion bodies of nuclear polyhedrosis viruses with second harmonic generation microscopy," *Opt. Express* **16**, 5602–5608 (2008).
27. E. Brown, T. McKee, E. diTomaso, A. Pluen, B. Seed, Y. Boucher, and R. K. Jain, "Dynamic imaging of collagen and its modulation in tumors *in vivo* using second-harmonic generation," *Nat. Med.* **9**, 796–800 (2003).
28. R. M. Williams, W. R. Zipfel, and W. W. Webb, "Interpreting second harmonic generation images of collagen I fibrils," *Biophys. J.* **88**, 1377–1386 (2005).
29. A. T. Yeh, N. Nassif, A. Zoumi, and B. J. Tromberg, "Selective corneal imaging using combined second-harmonic generation and two-photon excited fluorescence," *Opt. Lett.* **27**, 2082–2084 (2002).
30. S.-J. Lin, R.-J. Wu, H.-Y. Tan, W. Lo, W.-C. Lin, T.-H. Young, C.-J. Hsu, J.-S. Chen, S.-H. Jee, and C.-Y. Dong, "Evaluating cutaneous photoaging by use of multiphoton fluorescence and second-harmonic generation microscopy," *Opt. Lett.* **30**, 2275–2277 (2005).
31. T. A. Theodossiou, C. Thrasivoulou, C. Ekwobi, and D. L. Beckery, "Second harmonic generation confocal microscopy of collagen type from rat tendon cryosections," *Biophys. J.* **91**, 4665–4677 (2006).
32. K. Schenke-Layland, I. Riemann, U. A. Stock, and K. Konig, "Imaging of cardiovascular structures using near-infrared femtosecond multiphoton laser scanning microscopy," *J. Biomed. Opt.* **10**, 024017 (2005).
33. K. König, K. Schenke-Layland, I. Riemann, and U. A. Stock, "Multiphoton autofluorescence imaging of intratissue elastic fibers," *Biomaterials* **26**, 495–500 (2005).
34. T. Boulesteix, E. Beaurepaire, M.-P. Sauviat, and M.-C. Schanne-Klein, "Second-harmonic microscopy of unstained living cardiac myocytes: measurements of sarcomere length with 20-nm accuracy," *Opt. Lett.* **29**, 2031–2033 (2004).
35. S. V. Plotnikov, A. C. Millard, P. J. Campagnola, and W. A. Mohler, "Characterization of the myosin-based source for second-harmonic generation from muscle sarcomeres," *Biophys. J.* **90**, 693–703 (2006).
36. S. J. Wallace, J. L. Morrison, K. J. Botting, and T. W. Kee, "Second-harmonic generation and two-photon-excited autofluorescence microscopy of cardiomyocytes: quantification of cell volume and myosin filaments," *J. Biomed. Opt.* **13**, 064018 (2008).
37. S. Chaudhuri, H. Nguyen, R. M. Rangayyan, S. Walsh, and C. B. Frank, "A Fourier domain directional filtering method for analysis of collagen alignment in ligaments," *IEEE Trans. Biomed. Eng.* **34**, 509–518 (1987).
38. Y. Xia and K. Elder, "Quantification of the graphical details of collagen fibrils in transmission electron micrographs." *J. Microsc.* **204**, 3–16 (2001).
39. J. P. Marquez, "Fourier analysis and automated measurement of cell and fiber angular orientation distributions," *Int. J. Solids Struct.* **43**, 6413–6423 (2006).
40. S. Plotnikov, V. Juneja, A. B. Isaacson, W. A. Mohler, and P. J. Campagnola, "Optical clearing for improved contrast in second harmonic generation Imaging of skeletal muscle," *Biophys. J.* **90**, 328–339 (2006).

41. P. Matteini, F. Ratto, F. Rossi, R. Cicchi, C. Stringari, D. Kapsokalyvas, F. S. Pavone, and R. Pini, "Photothermally-induced disordered patterns of corneal collagen revealed by SHG imaging," *Opt. Express* **17**, 4868–4878 (2009).
42. C. Bayan, J. M. Levitt, E. Miller, D. Kaplan, and I. Georgakoudi, "Fully automated, quantitative, noninvasive assessment of collagen fiber content and organization in thick collagen gels," *J. Appl. Phys.* **105**, 102042 (2009).
43. MATLAB, http://www.mathworks.com/products/matlab
44. S.-W. Chu, S.-P. Tai, T.-M. Liu, C.-K. Sun, and C.-H. Lin, "Selective imaging in second-harmonic-generation microscopic with anisotropic radiation," *J. Biomed. Opt.* **14**, 010504 (2009).
45. G. Andreas, K. Gerhard, and W. Gerald, "Probabilistic aspects of entropy," Chap. 3 in *Entropy–Princeton Series in Applied Mathematics*, pp. 37–52, Princeton University Press, Princeton, NJ (2003).